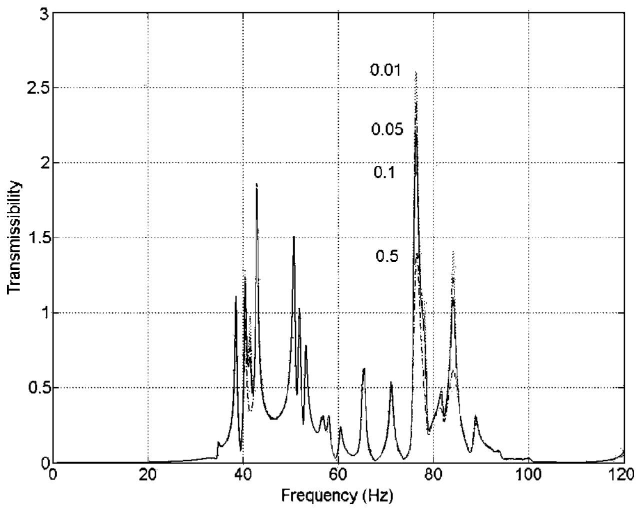

Fig. 4 Influence of the damping on the transmissibility in the horizontal direction.

where D_V is the displacement on the top of the PAF in the vertical direction and $D_{\text{base}-\text{V}}$ is the displacement at the bottom of the PAF in the vertical direction. The definition of the horizontal transmissibility shown in Fig. 4 is

$$T_V = \left| \frac{D_H}{D_{\text{base}-\text{V}}} \right| \tag{5}$$

where D_H is the displacement on the top of the PAF in the horizontal direction.

When the loss factor is about 0.1, the dynamic environment of the new launch vehicle is better than that of the old type, and the satellite is qualified for being launched. Together with some other factors such as launch cost and technical feasibility, the loss factor was finally chosen as 0.1. By this damping treatment the satellite was qualified to be launched with the new launch vehicle.

Conclusions

The WSVI is a direct and effective approach toward the improvement of the dynamic environment that a launch vehicle can provide to its payload. Although effect of adding damping to the PAF for generating a hard ride is not as good as other methods, it is cheap and fast, especially when there is strict constraint on the spacecraft room inside the fairing.

Coupling analysis is essential in designing the WSVI, especially when the damping is involved. In the primary design for choosing the overall stiffness and damping of the isolation the study can be carried out with a simplified model, as shown in Fig. 1.

The soft ride can significantly decrease the transmissibility. Although in the case of soft ride, the damping of the isolator will increase the transmissibility, because of the coupling effect damping can have an important contribution to the vibration isolation. Moreover, damping is essential to the isolation of shocks. With a hard ride the damping can effectively reduce the vibration amplitude of the isolated structure at resonance frequencies.

References

[1]Johnson, D. C., Wilke, S. P., and Grosserode, J. P., "Whole-Spacecraft Vibration Isolation System for the GFO/Taurus Mission," *SPIE Conference on Passive Damping and Isolation*, Vol. 3672, Society of Photo-Optical Instrumentation Engineers (International Society for Optical Engineering), 1999, pp. 175–185.

[2]Johnson, D. C., Wilke, S. P., and Darling, R. K., "Multi-Axis Whole-Spacecraft Vibration Isolation for Small Launch Vehicles," *SPIE Conference on Smart Structures and Materials*, Vol. 4331, Society of Photo-Optical Instrumentation Engineers (International Society for Optical Engineering), 2001, pp. 31–37.

[3]Nelson, F. C., "Vibration Isolation Review 2: Shock Excitation," *Shock and Vibration*, Vol. 3, No. 6, 1996, pp. 451–459.

[4]Lee-Glauser, G., and Ahmadj, G., "Vibration Isolation of Launch Vehicle Payload and Its Subsystem," *Journal of Aerospace Engineering*, Vol. 8, No. 1, 1995, pp. 1–8.

[5]Kim, S., Elliott, S. J., and Brennan, M. J., "Decentralized Control for Multichannel Active Vibration Isolation," *IEEE Transactions on Control Systems Technology*, Vol. 9, No. 1, 2001, pp. 93–100.

[6]Tao, J. S., Liu, G. R., and Lam, K. Y., "Design Optimization of Marine Engine-Mount System," *Journal of Sound and Vibration*, Vol. 235, No. 3, 2000, pp. 477–494.

[7]Sciulli, D., and Inman, D. J., "Isolation Design for a Flexible System," *Journal of Sound and Vibration*, Vol. 216, No. 2, 1998, pp. 251–267.

[8]Xiong, Y. P., Xing, J. T., Price, W. G., and Wang, X. P., "Hybrid Active and Passive Control of Vibratory Power Flow in Flexible Isolation System," *Shock and Vibration*, Vol. 7, No. 3, 2000, pp. 139–148.

[9]Haddad, W. M., Razavi, A., and Hyland, D. C., "Active Vibration Isolation of Multi-Degree of Freedom Systems," *Proceedings of the American Control Conference*, Vol. 4, 1997, pp. 3537–3541.

[10]Li, D. B., and Yam, L. H., "Modal Synthesis Method for Vibration Isolation Design of Massive Rotating Machines Resiliently Supported by an Elastic Structure," *Journal of Sound and Vibration*, Vol. 231, No. 1, 2000, pp. 233–245.

[11]Hsueh, W. J., "Analysis of Vibration Isolation Systems Using a Graphic Model," *Journal of Sound and Vibration*, Vol. 216, No. 3, 1998, pp. 399–412.

[12]Leung, Y. T., and Cheung, Y. K., "Dynamic Analysis of Frames by a Two-Level Finite Element Method," *Journal of Sound and Vibration*, Vol. 74, No. 1, 1981, pp. 1–9.

A. Berman
Associate Editor

Optimal Design of the Optical Pickup Suspension Plates Using Topology Optimization

Gil Ho Yoon* and Yoon Young Kim†
Seoul National University,
Seoul 151-742, Republic of Korea

I. Introduction

IN this work we deal with the design optimization of the suspension plates of a high-speed optical pickup used in DVDs or CD-ROMs. Figure 1 shows a typical pickup assembly with the bobbin and the suspension plates. The four suspension plates are made identical to minimize unwanted motions. The structural design issues and related references on this subject can be found in Kim et al.[1] and Kim and Lee.[2] The specific design target here is to increase the torsional eigenfrequency of the pickup as high as possible while keeping the focusing eigenfrequency between 25 and 35 Hz and the tracking eigenfrequency between 43 and 57 Hz. These frequency ranges are set to meet design constraints such as servocontrollability. To find an optimal plate shape, we employ the topology optimization methodology.[3,4] Specifically, the multiscale topology optimization method[5] will be used to enhance the solution efficiency.

Received 27 August 2002; revision received 25 March 2003; accepted for publication 27 March 2003.

*Graduate Student, School of Mechanical and Aerospace Engineering and National Creative Research Initiatives Center for Multiscale Design, Shinlim-Dong San 56-1, Kwanak-Gu; pilot@idealab.snu.ac.kr.

†Professor, School of Mechanical and Aerospace Engineering and National Creative Research Initiatives Center for Multiscale Design, Shinlim-Dong San 56-1, Kwanak-Gu; yykim@snu.ac.kr.

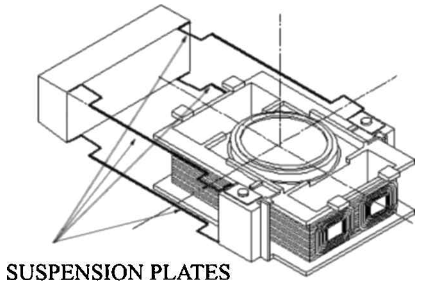

Fig. 1 Typical suspension plate-type pickup.

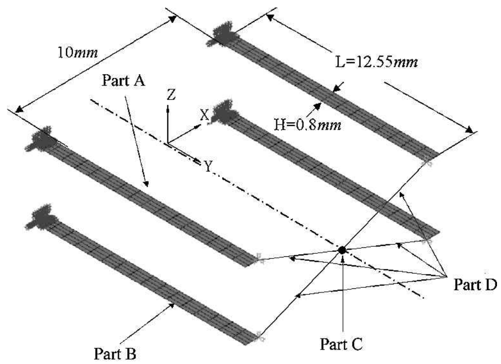

$$m_{Bobbin} = 0.5g$$

$$(\mathbf{I}_{Bobbin}) = \begin{pmatrix} 5.703 & 0 & 0 \\ 0 & 4.083 & -1.057 \\ 0 & -1.057 & 8.354 \end{pmatrix} g \cdot mm^2$$

Fig. 2 Finite element model of the baseline design consisting of four suspension plates and a bobbin: part A, upper suspension plates; part B, lower suspension plates; part C (bobbin center), concentrated mass with inertia; and part D, rigid link.

II. Modeling and Problem Formulation

In this research the shape and topology of the suspension plates in Fig. 1 will be optimized to maximize the twisting frequency f_{tw} while keeping the focusing f_{fc} and tracking f_{tr} frequencies in certain frequency ranges.

Maximize:

$$f_{\mathrm{tw}}$$

Subject to:

$$\left| f_{\mathrm{fc}} - f_{\mathrm{fc}}^{\mathrm{spec}} \right| \le \delta_{\mathrm{fc}}, \qquad \left| f_{\mathrm{tr}} - f_{\mathrm{tr}}^{\mathrm{spec}} \right| \le \delta_{\mathrm{tr}} \tag{1}$$

where the target values are denoted by "spec" and the permitted frequency ranges are specified by δ_{fc} and $\delta_{\mathrm{tr}}(f_{\mathrm{fc}}^{\mathrm{spec}} = 30$ Hz, $f_{\mathrm{tr}}^{\mathrm{spec}} = 50$ Hz, $\delta_{\mathrm{fc}} = 7$ Hz, $\delta_{\mathrm{tr}} = 7$ Hz). Because the bobbin can be modeled as a point mass[1,2] in the frequency range of interest, we can use the design optimization model shown in Fig. 2. (For suspension plates, Young's modulus = 100 GPa, Poisson's ratio = 0.33, and thickness = 0.1 mm.) The suspension plate is discretized by 4×16 four-node shell elements, so that the minimum width of the plate will be maintained as 200 μm.

For the topology optimization of the suspension plates, the density variable $\rho_e (0 < \rho_e \le 1)$ is assigned to each finite element, and the element mass m_e and the elastic coefficient E_e are penalized by solid isotropic material with penalization (SIMP)[6]:

$$E_e(\rho_e) = \rho_e^{\mu} E_0, \qquad v = v_0, \qquad m_e = \rho_e V_e$$

$$0 < \rho_e \le 1, \qquad 1 \le e \le N_e \tag{2}$$

where N_e is the number of finite elements and V_e the corresponding element volume. We choose $\mu = 3$ as the values of μ between two and three usually give satisfactory results.[4–6] When the objective functions and constraint equations are specified and the penalization scheme is selected, one can carry out topology optimization using the density variables ρ_e as the design variables.

The multiscale topology optimization method we employ in this work has been used to realize progressive design[5,7] and to handle some numerical instability problems[8–10] such as checkerboard pattern formation. This method also can be used to improve solution convergence in some applications. Because of the space limitation, we do not explain either the standard single-scale method or the multiscale method. For single-scale eigenvalue topology optimization see Kim and Kim,[11] and for multiscale topology optimization see Kim and Yoon.[5]

III. Mode-Tracking Issue in Multiple Eigenvalue Problems

Unlike static problems, optimization problems involving mutiple eigenvalues might suffer from mode switching, which often causes serious difficulties in solution convergence. To handle this situation satisfactorily, techniques such as mode-tracking schemes[11,12] should be used. In this work we employ the modal-assurance-criterion (MAC)-based mode-tracking scheme[11] that traces the desired modes by examining the MAC values. The definition of MAC is

$$\mathrm{MAC}(\boldsymbol{\Phi}_a, \boldsymbol{\Phi}_b) = \frac{\left| \boldsymbol{\Phi}_a^T \boldsymbol{\Phi}_b \right|^2}{\left(\boldsymbol{\Phi}_a^T \boldsymbol{\Phi}_a \right)\left(\boldsymbol{\Phi}_b^T \boldsymbol{\Phi}_b \right)} \tag{3}$$

where $\boldsymbol{\Phi}_a$ and $\boldsymbol{\Phi}_b$ denote two mode shapes of interest. MAC varies between zero and one, and it gives a value close to one if two modes are similar. If the MAC value is greater than a certain threshold number (say, 0.8), the two modes are declared the same.

At the beginning of optimization, the reference modes $\boldsymbol{\Phi}_a$ are predetermined from the baseline design, and the modes $\boldsymbol{\Phi}_b$ obtained during the optimization process are substituted into Eq. (3). Figure 3 shows three mode shapes $\boldsymbol{\Phi}_a$ obtained for the baseline design. Though the baseline structure can be significantly different from the structures appearing during optimization, the MAC-based method is valid because the modal characteristics of the focusing, tracking, and twisting modes do not change.

IV. Numerical Results

Before providing the present topology optimization result, it is worth demonstrating the difficulty of modifying the existing suspension plates by size optimization. Figure 4 shows the finite element model of a pickup having rectangular-bend suspension plates developed earlier.[1,2] By changing the dimensions of rectangular-bend suspension plates alone, it is difficult or impossible to find a pickup system satisfying the design goal; for instance, typical eigenfrequencies of the pickup system obtained by straightforward size optimization are $f_{\mathrm{fc}} = 40.44$ Hz, $f_{\mathrm{tr}} = 43.08$ Hz, and $f_{\mathrm{tw}} = 98.2$ Hz. As shall be seen later, the topology optimization method yields a much higher twisting eigenfrequency.

Figure 5a shows the optimized suspension plate by the multiscale topology optimization method after 28 iterations. (The initial values of $\rho_e = 0.5$ are used.) To guarantee the symmetry of the suspension system, the design variables of the four plates are appropriately linked; all independent design variables are assigned to one of the four plates. Unlike the existing suspension plates having abrupt shape changes such as rectangular bends, the present suspension plate has gradually changing thickness variation. The result in Fig. 5a is not completely free from gray regions, but it might be sufficient to identify an initial design. Because there is no mass constraint in the present problem, the postprocessing of the result in Fig. 5a is less complicated. Figure 5b shows the design layout after dropping elements whose density values are under 0.3. Figure 5c is the final design layout postprocessed from Fig. 5b.

The eigenfrequencies of the pickup having the suspension plates shown in Figs. 5a and 5c are tabulated in Table 1. In comparison with the typical result by the size optimization, the present optimized design has a much higher twisting eigenfrequency. Though

Table 1 Eigenfrequencies for the optimized designs shown in Figs. 5a and 5c

Model	Focusing, Hz	Tracking, Hz	Twisting, Hz
Fig. 5a	35.0	56.9	177.5
Fig. 5c	35.6	44.3	137.4

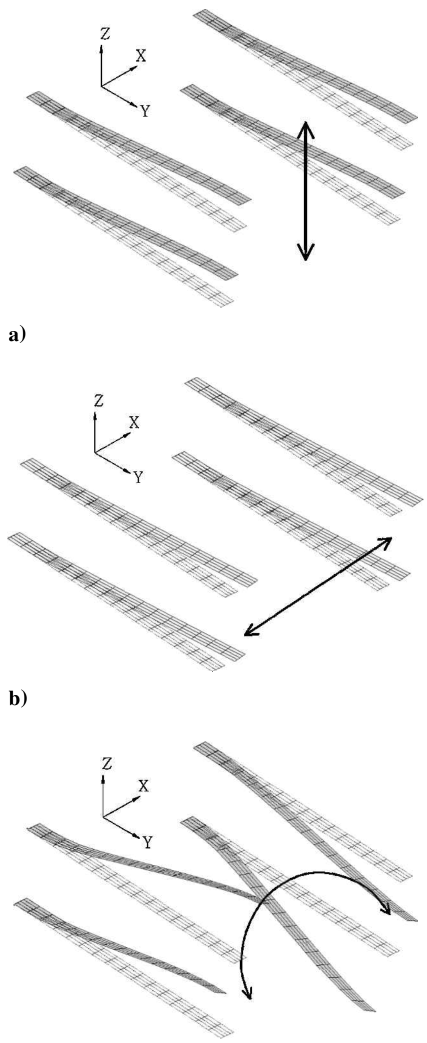

Fig. 3 Three fundamental mode shapes of the baseline bobbin-suspension system: a) focusing, b) tracking, and c) twisting mode shape (↔, motion directions).

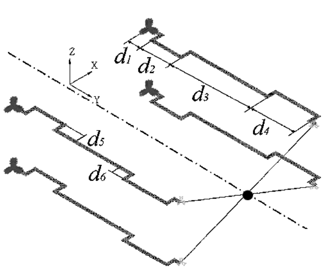

Fig. 4 Finite element model of a pickup having rectangular-bend suspension plates.[1,2] The design variables for size optimization are denoted by d_i ($i = 1 \sim 6$).

Fig. 5a Optimized result after 28 iterations.

Fig. 5b Postprocessed result after dropping elements whose densities are under 0.3.

Fig. 5c Finally proposed suspension plate.

the postprocessing somewhat deteriorates the original performance, the numerical result for the plate in Fig. 5c is still satisfactory.

V. Conclusions

The topology optimization method is successfully applied to find an optimal shape of suspension plates of optical pickups for high-speed DVDs or CD-ROMs. The twisting eigenfrequency has been maximized while the focusing and tracking eigenfrequencies are kept in the prescribed frequency range. Through this design problem we have demonstrated that the topology optimization method yields practically useful results, which are otherwise difficult to obtain.

References

[1] Kim, Y. Y., Kim, J. Y., and Han, J. Y., "A New Optical Pickup Suspension Design," *International Journal of Solids and Structures*, Vol. 36, 1999, pp. 2541–2556.

[2] Kim, Y. Y., and Lee, H. C., "Analytic Solutions for Fundamental Eigenfrequencies of Optical Actuators in Six Motion Directions," *International Journal of Solids and Structures*, Vol. 38, 2001, pp. 1327–1339.

[3] Bendsoe, M. P., and Kikuchi, N., "Generating Optimal Topologies in Structural Design Using a Homogenization Method," *Computer Methods in Applied Mechanics and Engineering*, Vol. 71, 1988, pp. 197–224.

[4] Suzuki, K., and Kikuchi, N., "A Homogenization Method for Shape and Topology Optimization," *Computer Methods in Applied Mechanics and Engineering*, Vol. 93, 1991, pp. 291–318.

[5] Kim, Y. Y., and Yoon, G. H., "Multi-Resolution Multi-Scale Topology Optimization—A New Paradigm," *International Journal of Solids and Structures*, Vol. 37, 2000, pp. 5529–5559.

[6] Bendsøe, M. P., and Sigmund, O., "Material Interpolation Schemes in Topology Optimization," *Archive of Applied Mechanics*, Vol. 69, 1999, pp. 635–654.

[7] Mallat, S., *A Wavelet Tour of Signal Processing*, Academic Press, New York, 1998.

[8] Yoon, G. H., Kim, Y. Y., Bendsøe, M. P., and Sigmund, O., "Hinge-Free Topology Optimization with Embedded Translation-Invariant Differentiable Wavelet Shrinkage," *Structural and Multidisciplinary Optimization* (to be published).

[9] Earmme, T. M., "The Role of the Wavelet Basis in Multiscale Topology Optimization," M. S. Thesis, School of Mechanical and Aerospace Engineering, Seoul National Univ., Seoul, Republic of Korea, Feb. 2001.

[10] Poulsen, T. A., "Topology Optimization in Wavelet Space," *International Journal for Numerical Methods in Engineering*, Vol. 53, 2002, pp. 567–582.

[11] Kim, T. S., and Kim, Y. Y., "Mac-Based Mode-Tracking in Structural Topology Optimization," *Computers and Structures*, Vol. 74, 2000, pp. 375–383.

[12] Eldred, M. S., Venkayya, V. B., and Anderson, W. J., "Mode Tracking Issues in Structural Optimization," *AIAA Journal*, Vol. 33, No. 10, 1995, pp. 1926–1933.

A. Berman
Associate Editor